Bull. Astr. Soc. India (2003) 31, 303–308

Dynamics of Limb Flare and Associated Primary and Secondary Post Flare Loops

Wahab Uddin*, Bhuwan Joshi, Ramesh Chandra, Anita Joshi
State Observatory, Manora Peak, Naini Tal 263 129

Abstract. In this paper we present the analysis of M 1.8 class (GOES SXR) limb flare and associated post flare loops of 2 May, 2001 which erupted on the west limb in NOAA 9433 (N15, W88). The flare started at around 00:32 UT from a small mound of twisted loops. When we started Hα observations at 00:52 UT the flare was in decay phase enveloped by highly sheared/twisted post flare loops which we call as primary post flare loops. The unique feature of this flare was that a new system of loops were developed when the primary loops were almost decaying. We call these newly formed loops as secondary loops. The main aim of the paper is to study the dynamics of the Hα flare/post flare loops and to understand how the magnetic field gets relaxed from highly sheared/twisted stage to a simplified potential field. We have discussed the nature of temporal behavior of the temperature and emission measure of the flare. The post flare condensation and formation of secondary loops has also been studied in this paper. The flare was also associated with SXR, HXR and MW emissions.

Keywords : flare loops - limb flare - magnetic field

1. Introduction

Limb flares and associated post flare loops give us a unique opportunity to study the three dimensional magnetic structures within an active region. These post flare loops, which are clearly the fundamental part of flare itself, are widely believed to be the physical evidence of on-going magnetic field line reconnection during the gradual phase of two ribbon flares (See reviews by Svestka, 1989). The magnetic reconnection keeps forming new loops, which are filled with hot plasma by chromospheric evaporation, cool down either quickly, in a few minute, or slowly, over 1 or 2 hours, depending on their density, to appear eventually as Hα loops (Schmieder et al., 1987; White et al., 2002; Reeves and Warren, 2002).

*E-mail: wahab@upso.ernet.in

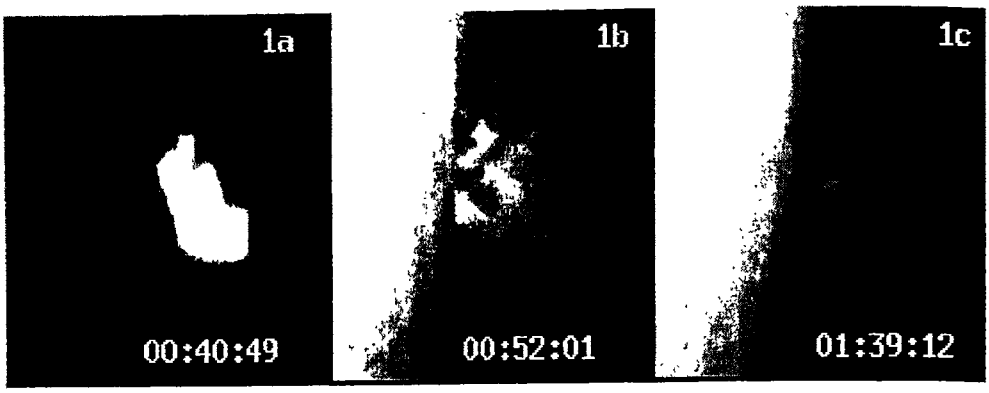

Figure 1. (a) *Hα* filtergram of flare observed from Holloman observatory, New Maxico. (b) and (c) present *Hα* filtergrams of primary and secondary post flare loops observed from State observatory, Nainital. The field of view is 125″ × 125″. North is up and west is right.

The Hα flare loops appear generally as dark loops during the gradual phase of a flare; viewed on the limb they may appear as loops in emission, reaching 50,000 km. They may create a system of quasi-steady arched lasting upto several hours. Large down flows are observed along the legs of the loops with deceleration by comparing free fall motion (Schmieder, 1991). In large flares changes in the large scale arrangement of the active region can typically be observed before and after the flare phase. The active filament that often lies along a magnetic neutral line rises and lifts off, the two ribbons appear visible in Hα one to each side of the neutral line. The flare loops are the part of an arcade which links the two ribbons. The Hα filtergrams are very useful to derive morphological properties of the loops. In this paper we describe the morphology and dynamics of M1.8 class limb flare and associated flare loop system of May 2, 2001.

2. Observations

A huge system of post flare loops was developing on the west limb on May 2, 2001 which was associated with M 1.8 class flare. The flare started around 00:32:19 UT. When we started our observations around 00:52 UT the flare was running in its decay phase enveloped with very complex post flare loop system. The system of loops was well observed by us using 15 cm f/15 coude' refractor at the State Observatory, Nainital. The telescope is equipped with Bernhard Halle *Hα* (6563 Å/0.5 Å) filter and CCD (512 × 512) Photometrics camera system. The images have the pixel resolution of 0.65″. To study the flare before 00:52 UT, we have used the *Hα* data of Holloman Observatory, New Mexico (http://sec.noaa.gov/solar_images). To study the temporal evolution of temperature and emission measure we have used GOES 8 SXR data. The resolution of these images is about 0.8″ per pixel. The reduction work was done using IRAF and IDL softwares.

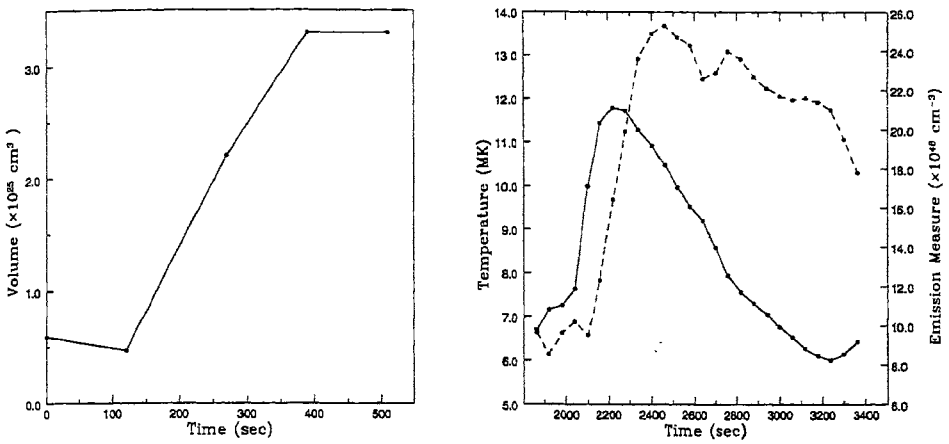

Figure 2. (a) Plot of volume of the flare versus time (Left). (b) Figure on the right shows the plot of temperature (solid line) and emission measure (dashed line) versus time.

3. Analysis and Results

The *Hα* filtergrams of the flare taken by Holloman Observatory during 00:32 to 00:41 UT show that the flare started as a reconnection of low lying two loop system above the limb. At 00:34 UT there was a sudden increase in brightness near the loop top. After 00:34 UT the flare structure changed rapidly. The figure 1a shows the *Hα* filtergram of the flare when it was running in its maximum phase. The hot material pumped along the loop. As a result of this the helically twisted flux tube gets stretched and detwisted resulting in the increase of the flare volume. The change in helical structure is clearly visible during flare evolution which indicates the relaxation of sheared/twisted magnetic field structure. We have calculated the volume of flare in different stages. Figure 2a shows the plot of the volume of flare versus time. At 00:40 UT, when the flare was in its maximum phase, the estimated volume was about 3.3×10^{25} cm^3. During the rising phase of the flare the estimated velocity of the flare material was approximately 200 km/sec and its estimated kinetic energy was about 10^{28} ergs. The total flare energy may be higher. The flare shows similar evolutions in high temperature (10^6 K) region i.e. in SXR and HXR (observed by Yohkoh) and 17 GHz and 34 GHz MW (observed by Nobeyama). The effective temperature (T_{eff}) and emission measure (EM) of the flare are calculated from GOES 8 SXR data by the ratio technique given in Thomas, Starr and Crannell (1985). Figure 2b shows the plot of temperature and EM versus time. The estimated maximum values of T_{eff} and EM are 11.79 MK and 2.53×10^{49} cm^{-3} respectively. Earlier statistical studies show that for the very faint X-ray class A flare the emission measure can be as small as 1×10^{46} cm^{-3} while for the bright X-ray class X2 flares it can approach 1×10^{50} cm^{-3} (Feldman et al., 1996). Our calculated values of EM are in good agreement with these values. It is obvious from this figure that the temperature reached to its maximum value before the EM. The comparison of plots shown in figure 2b and 2a shows that

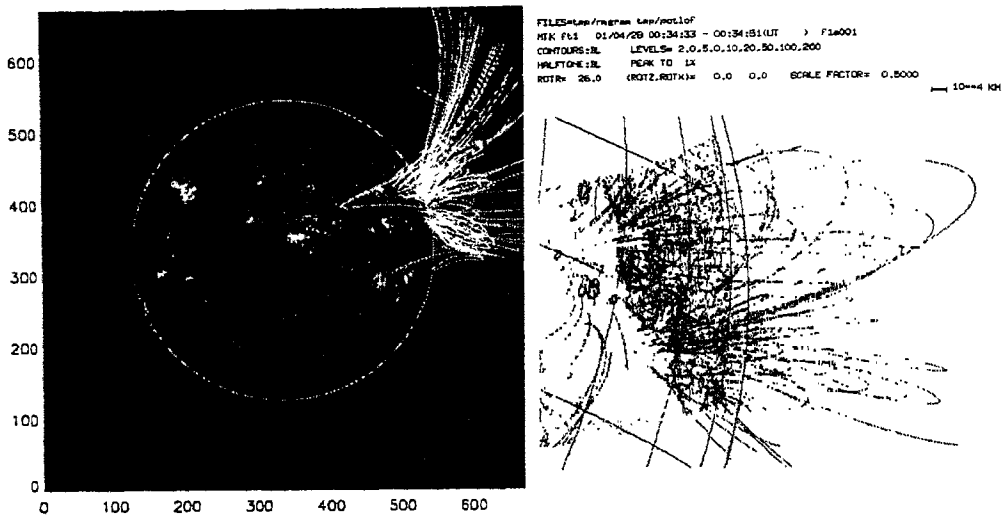

Figure 3. Potential field line extrapolation from the magnetogram of SOHO/MDI (Left) and Mitaka, Japan (Right) showing the similarity of the potential field to the post flare loops.

the times of greatest temperature enhancement are the times of most rapid growth of the emission measure during which the volume of the flare also increased very rapidly. This suggests a model in which the flare begins as a small hot region and undergoes rapid expansion and cooling (Milkey et al., 1971).

The Hα filtergrams of post flare loop system observed by us after 00:52 UT show that the flare loop system consists of many loops. The structures of the loop system are very complex and some loops are highly inclined. A number of loops are overlapped and inlaid on one another. The movie of the images between 00:52 UT and 01:16 UT shows that the hot plasma is moving from north-west foot-point to south-east foot-point. By the comparison of images during this period we find that the structure becomes simplified and the number of loops decreases . These changes in the structure of post flare loops reflect that magnetic field gets relaxed from highly sheared/twisted into almost potential field. On the other hand the height of the loop system remains almost constant (45,000 km). The long lived structure of post flare loop system is an evidence of on going reconnection of magnetic field lines which releases the energy continuously. We call these loops as primary loops. Figure 1b presents one such Hα filtergram of primary loop system. After 01:16 UT the brightness of the loop system decreases significantly. The potential field extrapolation based on the magnetogram of SOHO/MDI and Mitaka, Japan is shown in figure 3 (left and right respectively). The figure 3 (left) shows the potential fields as derived from the observations on 1 May 2001. This active region was not observed from Mitaka on 1 and 2 May, 2001 when it was close the limb, therefore we have derived the potential field from the observations of 28 April, 2001 and then rotated the field lines by 26° . Figure 3 (Right) shows that after this rotation how the field lines will appear on 30 April, 2001 or so. The comparison of

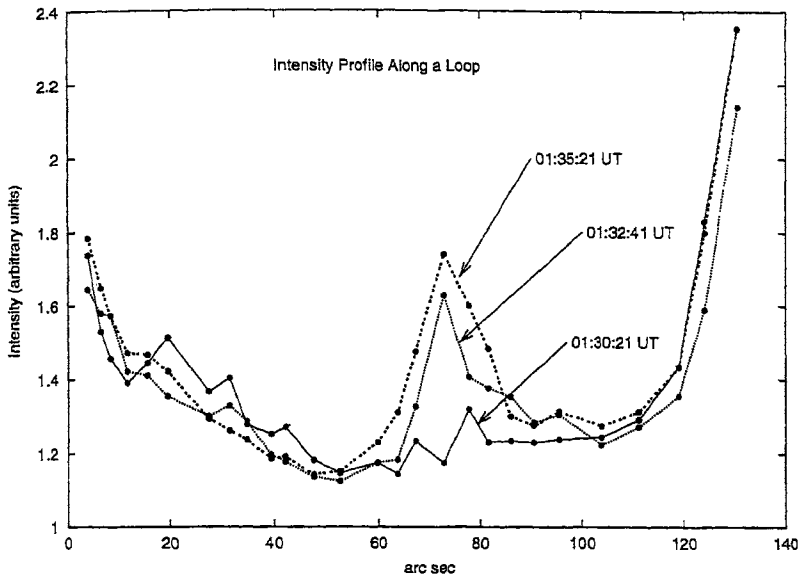

Figure 4. Intensity profile along the third secondary loop for three different times

post flare loop structure (cf. Figure 1b and 1c) and the potential field extrapolation (cf. Figure 3) shows that the loops apparently appeared to follow the potential field lines.

Some unusual changes take place after around 01:10 UT. When the primary loop system was about to disappear, a new system of loops started to develop. We call this newly formed system of loops as secondary loops. The examination of images between 01:10 UT to 01:50 UT, reveals that this new loop system consists of three loops which formed one after the another. Out of these three loops the third one was the most complex which consists of bundle of loops (cf. figure 1c). In all the three cases the material was pumped along the loops from its north-west foot-point and fell into south-east foot-point. The material was ejected in the form of highly fragmented blobs and then it condensed near the loop top. The maximum height of these loops were 33,976 km, 33,033 km, 31,145 km respectively. We estimated the velocity of downward motion of the condensed material. The average velocity of falling blobs came out to be about 87.82 km/sec, 93.04 km/sec and 81.64 km/sec respectively in three loop systems. These values are in good agreement with with those expected from the simplest model possible: a free-fall motion along a stationary circular loop. We also calculated the total mass of three loop systems (mass of plasma or material transferred from one foot point to other) by making the assumption that the average mass density of the loop material is of the order of 10^{-11} gm cm^{-3}. The mass of the three loop systems turned out to be 5.28×10^{15} gm, 3.72×10^{15} gm and 3.38×10^{16} gm respectively.

The inhomogeneity of the primary and secondary loops appear clearly in Hα filtergrams. The loops are visible when they are filled with material. The figure 4 shows the brightness

inhomogeneity of the third secondary loop system in which we have plotted a curve between the intensity along the loop versus length of the loop (in arc sec) from south-east foot-point to north-west footpoint for different times. The condensation started near the loop top which is shown by arrows in figure 4. It is clear from the figure that the condensation increases with time while the material moves towards south-east foot-point. This Hα inhomogeneities may be due to thermal instability during the condensation process or instability due to turbulence during the reconnection in an MHD model (Schmieder et al., 1995).

4. Acknowledgement

The authors are grateful to Prof. Jagdev Singh for valuable discussions. We are thankful to Prof. T. Sakurai and Dr. Y. Liu for providing us computed potential field of flaring region. The authors would like to thank an anonymous referee for useful comments.

References

Feldman, U., Doschek, G.A., Behring, W.E., Phillips, K.J.H., 1996, Astrophys. J., 460, 1034.

Milkey, R.W., Blocker, N.K., Chambers, W.H., Fehlau, P.E., Fuller, J.C., Kunz, W. E., 1971, Solar Phys., 20, 400.

Reeves, K.K., Warren, H., P., 2002, ApJ, 578, 590.

Schmieder, B., 1991, Eruptive Solar Flares, Eds. Z. Svestka, B. V. Jackson, M. E. Machado, Springer Verlag, p 124.

Schmieder, B., Forbes, T.G., Malherbe, J.M., Machado, M.E., 1987, Astrophys. J., 317, 956.

Schmieder, B., Heinzel, P., Wiik, J.E., Lemen, J., Anwar, B., Kotrc, P., Hiei, E., 1995, Solar Phys., 156, 337.

Svestka, Z., 1989, Solar Phys., 121, 399.

Thomas, R.J., Starr, R., Crannell, C.J., 1985, Solar Phys., 95, 323.

White, S.M., Kundu, M.R., Garaimov, V.I., Yokoyama, T., Sato, J., 2002, ApJ, 576, 505.